Biophysical Chemistry, 32 (1988) 57–72
Elsevier

BPC 01311

Fluorescence properties of cholestatrienol in phosphatidylcholine bilayer vesicles

Friedhelm Schroeder [a], G. Nemecz [a], E. Gratton [b], Y. Barenholz [c] and T.E. Thompson [c]

[a] *Division of Pharmacology and Medical Chemistry, College of Pharmacy, and Department of Pharmacology and Cell Biophysics, College of Medicine, University of Cincinnati Medical Center, Cincinnati, OH 45267-0004,* [b] *Laboratory for Fluorescence Dynamics, Department of Physics, University of Illinois at Urbana-Champaign, Urbana, IL 61801 and* [c] *Department of Biochemistry, University of Virginia School of Medicine, Charlottesville, VA 22908, U.S.A.*

Received 5 February 1988
Accepted 18 July 1988

Cholesterol; Cholestatrienol; Model membrane; Fluorescence; Lifetime distributional analysis; Small unilamellar vesicle

The fluorescent sterol $\Delta^{5,7,9,(11)}$-cholestatrien-3β-ol (cholestatrienol) was incorporated into 1-palmitoyl-2-oleoyl-phosphatidylcholine (POPC) small unilamellar vesicles (SUV) with and without cholesterol in order to monitor sterol-sterol interactions in model membranes. Previously another fluorescent sterol, dehydroergosterol (F. Schroeder, Y. Barenholz, E. Gratton and T.E. Thompson, Biochemistry 26 (1987) 2441), was used for this purpose. However, there is some concern that dehydroergosterol may not be the best analogue for cholesterol. Fluorescence properties of cholestatrienol in POPC SUV were highly sensitive to cholestatrienol purity. The fluorescence decay of cholestatrienol in the POPC SUV was analyzed by assuming either that the decay is comprised of a discrete sum of exponential components or that the decay is made up of one or more component's distribution of lifetimes. The decay for cholestatrienol in POPC SUV analyzed using distributions had a lower χ^2 value and was described by a two-component Lorentzian function with centers near 0.86 and 3.24 ns, and fractional intensities of 0.96 and 0.04, respectively. Both distributions were quite narrow, i.e., 0.05 ns full-width at half-maximum peak height. It is proposed that the two lifetime distributions are generated by separate continua of environments for the cholestatrienol molecule described by different dielectric constants. In the range 0–6 mol% cholestatrienol, the cholestatrienol underwent a concentration-dependent relaxation. This process was characterized by red-shifted absorption and maxima and altered ratios of absorption and fluorescence excitation maxima. Fluorescence quantum yield, lifetime, steady-state anisotropy, limiting anisotropy and rotational rate remained constant. In contrast, in POPC vesicles containing between 6 and 33 mol% cholestatrienol, the fluorescent cholestatrienol partially segregated, resulting in quenching. Thus, below 6 mol% cholestatrienol, the cholestatrienol appeared to behave in part as monomers exposed to some degree to the aqueous solvent in a sterol-poor domain within POPC bilayers. Since the lifetime did not decrease above 6 mol% cholestatrienol, the fluorescence at high mol% values of cholestatrienol was due to cholestatrienol in the sterol-poor domain. The fluorescence intensity, quantum yield, steady-state anisotropy, and limiting anisotropy of cholestatrienol in the sterol-poor domain decreased to limiting, nonzero values while the rotational rate increased to a limiting value. Thus, the sterol-poor domain became more disordered when it coexisted with the sterol-rich domain. In POPC vesicles containing 3 mol% cholestatrienol plus increasing mol% cholesterol the two sterols codistributed, since fluorescence quenching was not observed. Above 6 mol% total sterol the cholestatrienol was sensitive to sterol motional properties in the laterally segregated sterol-rich domain. The sterol-rich domain became more rigid with increasing cholesterol content of the POPC SUV. The data are consistent with the presence of a relatively ordered sterol-rich domain and a relatively sterol-poor polarity-sensitive domain coexisting in fluid-phase phospholipid vesicles. In conclusion, cholestatrienol and dehydroergosterol both appear to be sensitive probe molecules for monitoring cholesterol dynamics in membranes.

Correspondence address: F. Schroeder, Division of Pharmacology and Medical Chemistry, College of Pharmacy, and Department of Pharmacology and Cell Biophysics, College of Medicine, University of Cincinnati Medical Center, Cincinnati, OH 45267-0004, U.S.A.

Abbreviations: POPC, 1-palmitoyl-2-oleoylphosphatidylcholine; SUV, small unilamellar vesicles; cholestatrienol, $\Delta^{5,7,9(11)}$-cholestatrien-3β-ol.

1. Introduction

Cholesterol has a central role in modulating the structure and properties of biological membranes. Elucidation of cholesterol-cholesterol interactions as well as the interactions of cholesterol with other membrane components includes cholesterol lateral phase separation, and cholesterol-phospholipid and cholesterol-protein interactions [1]. Previously, identification of suitable probe molecules which, when inserted into membranes, accurately mimic the behavior of cholesterol was a major difficulty. More recently, fluorescent analogues of cholesterol such as dehydroergosterol have been utilized [1–3]. Although dehydroergosterol closely resembles ergosterol in structure, is nontoxic to cultured cells [4,5] and microorganisms [6,7] and is even biologically synthesized [8,9], there is some concern that it may not be the best analogue of cholesterol. Dehydroergosterol is oxidized poorly by cholesterol oxidase [4], more dehydroergosterol than cholesterol is required to abolish the phase transition of dipalmitoylphosphatidylcholine [4], and dehydroergosterol reduces the permeability of egg phosphatidylcholine vesicles less well than cholesterol [9]. In addition, side chain alkylated derivatives similar to dehydroergosterol are absorbed more slowly by the intestinal brush border [10]. In contrast, $\Delta^{5,7,9(11)}$-cholestatrien-3β-ol, another fluorescent sterol, more closely resembles cholesterol in structure than dehydroergosterol. Cholestatrienol is highly incorporated into LM fibroblast membranes without detrimental effect on the activity of cholesterol-sensitive enzymes such as $(Na^+ + K^+)$-ATPase and 5′-nucleotidase (F. Schroeder, unpublished observation). This fluorescent sterol has also been used to investigate the properties of cholesterol in very low density lipoproteins, low density and high density lipoproteins, red blood cell membranes (reviewed in ref. 1) and liposomes [6]. However, problems of instability and decomposition have hampered the use of cholestatrienol [6] in contrast to the more stable dehydroergosterol [11], as a fluorescent analogue of cholesterol. The problems of cholestatrienol instability have recently been resolved by HPLC purification of the cholestatrienol [12].

In this paper, we report the use of cholestatrienol to investigate sterol-sterol and sterol-phospholipid interactions in 1-palmitoyl-2-oleoylphosphatidylcholine (POPC)[1] small unilamellar vesicles (SUV). In particular, fluorescence lifetime analysis in combination with multifrequency phase and modulation spectroscopy allows resolution of sterol heterogeneity in POPC SUV. Previously, fluorescence decay of probe molecules such as diphenylhexatriene [13], parinaric acid [14–18], and dehydroergosterol [2,19] was represented by the sum of discrete exponential terms. However, more recent data indicate that a continuous distribution of decay rates may better describe the behavior of diphenylhexatriene [20,21] and parinaric acid [22] as opposed to a sum of discrete exponential terms. The basic rationale for such an approach, applied to cholestatrienol herein, is that the fluorescence probe molecules exist in a variety of positions perpendicular to the bilayer. In each position the probe may be characterized by a different lifetime value. In addition, the probes can undergo rapid translational and rotational motion.

2. Materials and methods

2.1. Reagents

1-Palmitoyl-2-oleoylphosphatidylcholine was purchased from Avanti Biochemicals (Birmingham, AL). Cholesterol was obtained from Mann Research Labs (New York, NY). These lipids were checked for purity by thin-layer chromatography and stored in sealed ampoules under N_2 at $-70\,^\circ C$. Cholestatrienol was synthesized and purified by HPLC as described previously [12]. Purity was confirmed by high-performance liquid chromatography, absorbance peak ratios, and comparison with cholestatrienol standards obtained from Frann Scientific (Columbia, MO).

2.2. Preparation of liposomes

Small unilamellar vesicles were prepared from POPC, cholesterol, and cholestatrienol exactly as described earlier [2]. Sonication was always performed under N_2 and above the phase transition temperature of the matrix phospholipid. The resulting SUV were separated from large vesicles

and multilamellar liposomes by differential ultracentrifugation for 2 h with a 40 Ti rotor and L7-55 ultracentrifuge (Beckman Instruments Fullerton, CA) as described earlier (23). The yield of POPC SUV in the supernatant in the presence of cholestatrienol decreased from approx. 60% at 0.5 mol% fluorescent sterol to 20% at 60 mol% sterol. This decrease was similar to that obtained in the formation of POPC SUV with increasing mol% cholesterol (data not shown) or with increasing mol% dehydroergosterol [2].

2.3. Lipid composition

The lipid composition of the SUV was examined in order to determine if the fluorescent sterol and cholesterol were incorporated into SUV in the same proportion (sterol : POPC) as was present in the starting mixture prior to sonication. The lipid composition of the SUV was determined as described earlier [2]. Stigmasterol or ergosterol was added as an internal standard prior to lipid extraction, and separation of neutral lipids from phospholipids by silicic acid chromatography [24]. Sterols were resolved both by analytical high-performance liquid chromatography [12] and by fluorescence analysis. In the latter method, the fluorescent cholestatrienol was quantitated by dissolving the neutral lipid fraction in ethanol, determining fluorescence or absorbance at 325 nm excitation (376 nm emission) as described below and comparing fluorescence intensities to those of a standard curve for cholestatrienol, also in ethanol. Cholestatrienol was incorporated into POPC SUV vesicles exactly in the same molar proportion as initially present prior to sonication. Plots of (measured mol% fluorescent sterol) vs. (starting mol% fluorescent sterol) were linear with a slope of 1.0 for cholestatrienol.

2.4. Fluorescence spectroscopy

Fluorescence parameters were measured as described earlier [2]. Light scattering was reduced by using dilute samples and by using Janos GG-375 or Schott KV-370 sharp cut-off filters in the emission system. Where light scattering was detectable, fluorescence intensities were corrected by subtracting the signal of an analogous vesicle preparation containing cholesterol instead of fluorescent sterol. The scattering correction was always less than 2%.

Steady-state fluorescence polarization, P, was determined in the L format using an SLM 4800 subnanosecond spectrofluorometer (SLM Instruments, Urbana, IL) modified to become a continuously variable (1–250 MHz) phase and modulation fluorometer (ISS, Urbana, IL). In determination of polarization, light scattering was reduced as described above. In addition, samples were serially diluted and polarization was measured and then extrapolated to zero absorbance [25,26]. The steady-state polarization, P, was corrected for excitation system-induced anisotropies [27].

2.5. Lifetime determination

Fluorescence lifetimes were measured by phase and modulation with two types of instruments: a multifrequency phase and modulation fluorometer (1–300 MHz), described elsewhere [28] or the SLM 4800 modified to 1–250 MHz (ISS, Urbana) described above. These instruments are based on the cross-correlation principle introduced by Spencer and Weber [29]. An He/Cd laser (model 4240NB, Liconix, Sunnyvale, CA), whose emission intensity at 325 nm was modulated sinusoidally with a Pockels cell, was the light source. The excitation and emission polarizers were set at 0° and the magic angle, 55°, respectively. Usually 14 modulation frequencies were utilized; at each frequency both phase and modulation of the fluorescence were determined with respect to a glycogen scatter solution or to a dimethyl-POPOP solution in ethanol. Scattered light was observed after it passed through an interference filter. Emission was observed through a Janos GG-375 or Schott KV-370 sharp cut-off filter. Data were collected with an ISS01 or ISS187 interface (ISS, Champaign, IL), by an IBM PC computer with math coprocessor and 20 MByte Seagate hard disk drive.

2.6. Lifetime nonlinear least-squares analysis

Fluorescence lifetime data analysis was performed with the above computer system using a

nonlinear least-squares routine for multiexponential fitting [30] and ISS01 software (ISS, Urbana). In the nonlinear least-squares method, the data were fitted to one or multiple exponential terms. In the latter case, each term was characterized by a lifetime τ and a fractional intensity f. The reduced chi squared (χ^2) parameter was utilized as described by Lakowicz et al. [20] to judge the quality of the fit. The error in each parameter was determined using a covariance matrix of errors [31]. The statistical analysis does not attribute physical significance to the parameters but only ensures that the data fit the model used.

2.7. Lifetime distributional analysis

Lifetime distributional analysis [32] was performed using ISS187 software (ISS, Urbana). The derivation for continuous distribution of lifetime values in frequency-domain fluorometry is reported elsewhere [20]. The data were fitted to several distributions including uniform, Gaussian and Lorentzian types. A Lorentzian continuous distribution gave the best fit (lowest χ^2). The Lorentzian function used was as follows:

$$f(\tau) = A/\left\{1 + \left[(\tau - C)/(W/2)\right]^2\right\} \quad (1)$$

where C is the center position of the distribution, W the width of the distribution at half-height, τ the lifetime and $f(\tau)$ represents the lifetime distribution. The constant A can be obtained from the normalization condition.

For both nonlinear least-squares and continuous distributional analysis the ISS187 program minimized the reduced χ^2 defined by:

$$\chi^2 = \sum\left\{\left[P_M - P_C)/S^P\right]^2 + \left[(M_M - M_C)/S^M\right]^2\right\}/(2n - f - 1) \quad (2)$$

where the subscripts C and M indicate the calculated and measured values, respectively, of phase and modulation, n is the number of frequencies employed, f the number of free parameters, and S^P and S^M the standard deviations of each phase and modulation determination, respectively. These standard deviations do not depend on the modulation frequency and are constant for each determination in phase fluorometry [33]. Therefore, they factor out in the χ^2 expression. The minimum value of χ^2 is not dependent on a common multiplicative factor.

2.8. Rotational analysis

Differential polarized phase fluorometry was used to obtain R, the rotational rate (radian/s) and r_∞, the limiting anisotropy, of cholestatrienol fluorescence in POPC SUV membranes according to the theory developed by Weber [34] and extended by Lakowicz et al. [35]. In the curve-fitting procedure, the values of r_0, the anisotropy in the absence of rotational motion, r_∞, and ϕ, the rotational correlation time (in ns), were floating parameters. The rotational rate (radian/s) equals $(6\phi)^{-1}$. This procedure utilized differential polarized phase and modulation data obtained at 14 frequencies between 10 and 250 MHz. Values of limiting anisotropy and rotational rate obtained thereby differ from those obtained by an earlier method [35,36]. In the earlier method only a single fixed frequency and a fixed $r_0 = 0.385$ (determined at 324 nm excitation according to the conditions described by Shinitzky and Barenholz [37]) were utilized. The He/Cd laser line at 325 nm was used as the cholestatrienol excitation wavelength.

Photobleaching is a potential problem associated with fluorescence measurement of many fluorophores. Over a 2 h time period, during which cholestatrienol in POPC SUV was exposed to strong ultraviolet light (450 W xenon lamp or He/Cd laser), the relative fluorescence intensity of the cholestatrienol (2 mol%) did not diminish significantly (99 ± 3 vs. 97 ± 4).

3. Results

3.1. Exponential lifetime analysis of cholestatrienol in POPC SUV

Multifrequency (1–250 MHz) phase and modulation spectrofluorometers were utilized to determine whether cholestatrienol has one or multiple lifetime components (table 1). The number of fluorescent lifetime components was highly depen-

Table 1

Effect of cholestatrienol purity on lifetime analysis in POPC SUV

Lifetime of 2 mol% cholestatrienol in POPC SUV was measured at 24°C by phase and modulation techniques at 5, 10, 20, 30, 40, 50, 60, 70, 80, 90, 100, 115, 120, 140 and 150 MHz. The number of lifetime components was determined by nonlinear least-squares analysis. F refers to fixed in the analysis. Fraction and α refer to fractional fluorescence and mole fraction, respectively.

Sample purity (%)	Component	Lifetime	Fraction	α	χ^2
86% (recrystallized)	1	0.503 ± 0.055	0.293 ± 0.026	0.852	4.31
	2	2.364 ± 0.309	0.181 ± 0.026	0.112	
	3	12.306 ± 1.019	0.270 F	0.032	
	4	86.000 F	0.256 F	0.004	
99% (HPLC)	1	0.829 ± 0.004	0.960 ± 0.003	0.99	1.80
	2	3.04 ± 0.270	0.040 ± 0.003	0.01	

dent on cholestatrienol purity with as many as four lifetime components being resolved by nonlinear least-squares analysis ($\chi^2 = 4.3$) of impure cholestatrienol in POPC SUV (86% purity as indicated by HPLC and by the mole fraction α, see table 1). Attempts at fitting the data for impure cholestatrienol to three, two, or one exponential components resulted in χ^2 values of 99, 198 and 411, respectively. It should be noted that for cholestatrienol a purity of 86% is typical for that achieved by standard recrystallization techniques [38] prior to the advent of preparative HPLC purification procedures [12,19]. In addition, we have shown elsewhere [12] that cholestatrienol purified by the recrystallization procedure [12] was very unstable such that at 24°C oxidation products in ethanol solution increased 6-fold in quantity within 2–3 h. In contrast, samples of cholestatrienol purified by preparative HPLC [12] were stable even after 3 months storage at −70°C in ethanol and up to 2 years as white crystals under N_2 at −70°C. The HPLC-purified cholestatrienol (99% pure according to HPLC and to α, the mole fraction, of lifetime component 1, see table 1) displayed two components near 0.829 and 3.04 ns ($\chi^2 = 1.8$), respectively, in POPC SUV (fig. 1). The theoretical curve for a two-exponential nonlinear least-squares fit and the actual data points coincide very well. However, the shorter lifetime component comprised 96% fractional intensity (99 mol%). Curve fitting to one lifetime component yielded a much larger χ^2 value of 32.

3.2. Distributional lifetime analysis of cholestatrienol in POPC SUV

The same set of data analyzed above using discrete exponential components was also analyzed by using a sum of two continuous distributions of lifetime values characterized by a Lorentzian shape centered at decay times C_1 and C_2 and having widths W_1 and W_2. Other distributions (uniform, Gaussian and single Lorentzian) were tested but fit the data less well. Cholestatrienol (fig. 2) showed a bimodal lifetime distribution with two components centered near 0.860 and 3.24 ns, respectively ($\chi^2 = 0.94$). The fractional intensity contributed by the two components was 96 and 4%, respectively. Both the major and minor components had a narrow distribution with a width at half-height of 0.05 ns. The mean reduced χ^2 for cholestatrienol was about 2-fold lower using the Lorentzian distributional analysis as compared to the sum-of-exponentials analysis (0.94 vs. 1.8). The major lifetime component of the Lorentzian distribution, with an average lifetime of 0.860 ns,

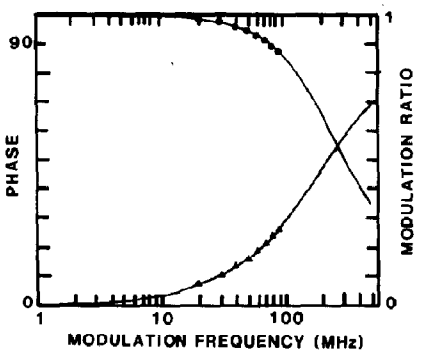

Fig. 1. Phase and modulation lifetime data for cholestatrienol in POPC SUV. Cholestatrienol (3 mol%) was incorporated into POPC SUV and phase angle (degrees, bottom curve) or modulation ratio (top curve) were obtained at 24°C as a function of modulation frequency (1–250 MHz). The solid lines indicate the best nonlinear least-squares two-component fit. The data points are the experimental values. χ^2 values for a one- and two-component fit were 31.9 and 1.80, respectively.

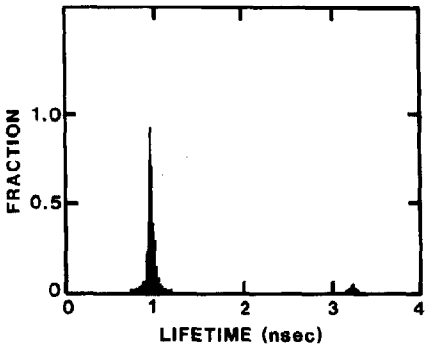

Fig. 2. Distributional analysis of cholestatrienol in POPC SUV. All conditions were as described in the legend to fig. 1, except that the data were fitted to a Lorentzian distribution.

was nearly indistinguishable from the major lifetime component (0.829 ns) obtained by using a double-exponential nonlinear least-squares analysis.

The second lifetime component of 3 mol% cholestatrienol in POPC SUV, although small in fractional fluorescence (0.04), was not due to an artifact or contaminant of the cholestatrienol preparation. The cholestatrienol used herein was of purity 99% or greater as determined by HPLC. In ethanol, below the cholestatrienol critical micellar concentration, only a single lifetime component at 0.392 ± 0.004 ns was resolved. Above the critical micellar concentration in ethanol a second component near 5 ns appeared, with increasing fractional intensity at higher cholestatrienol concentrations above the critical micelle concentration. In addition, the fractional intensity and width contributed by the minor component varied greatly with vesicle curvature. In multilamellar POPC vesicles, 3 mol% cholestatrienol also exhibited two lifetime components ($C_1 = 0.905$ ns, $C_2 = 2.675$ ns). However, the cholestatrienol fractional intensity due to C_2 increased from 0.040 in POPC SUV to 0.168 in POPC multilamellar vesicles. Likewise, the width of component C_2 (but not C_1) increased from 0.05 ns in POPC SUV to 0.174 ns in POPC multilamellar vesicles. In summary, both the exponential and distributional lifetime analysis are consistent with the presence of two discrete cholestatrienol components in POPC SUV.

3.3. Dependence of lifetime on cholestatrienol concentration

Multifrequency (1–250 MHz) phase and modulation spectrometers were utilized to determine

Table 2

Effect of increasing mol% cholestatrienol on lifetime analysis in POPC SUV [a]

mol% cholestatrienol	Lifetime analysis (ns)					
	Exponential (two component) [b]					
	τ_1	τ_2	F_1	χ^2		
2	0.829 ± 0.004	3.7 ± 1.3	0.96 ± 0.01	1.8		
4	0.885 ± 0.009	3.0 ± 1.7	0.96 ± 0.01	3.0		
10	0.818 ± 0.007	3.1 ± 1.3	0.98 ± 0.02	2.4		
50	0.901 ± 0.008	3.0 ± 1.9	0.99 ± 0.01	3.0		
	Lorentzian (two component) [c]					
	C_1	C_2	W_1	W_2	F_1	χ^2
2	0.860	3.24	0.05	0.05	0.96	0.94
4	0.880	3.10	0.05	0.05	0.97	1.90
10	0.921	–	0.05	–	1.00	1.29
50	1.155	–	0.05	–	1.00	2.51

[a] Lifetime of cholestatrienol in POPC SUV was measured at 24° C by phase and modulation techniques at 10, 20, 30, 40, 60, 70, 80, 90, 100, 115, 120, 130, 140 and 150 MHz. Values represent the mean ± S.E. ($n = 14$).

[b] τ_1, τ_2 and F_1 represent lifetime component 1, lifetime component 2 and fractional fluorescence of component 1, respectively, by nonlinear least-squares analysis.

[c] C_1, C_2, W_1, W_2, and F_1 represent the center of lifetime distribution 1 and 2, the peak width at half-height of distribution 1 and 2 and the fractional fluorescence of component 1, respectively, by continuous lifetime distributional analysis.

the effect of cholestatrienol concentration in POPC SUV on the distribution and lifetime of cholestatrienol lifetime components (table 2). Nonlinear least-squares analysis for a two-lifetime fit showed χ^2 values below 3 for 2–50 mol% cholestatrienol in POPC vesicles. The data for 2 mol% cholestatrienol fit a nonlinear least-squares two-component lifetime analysis at 0.829 ± 0.004 ns (fractional intensity, 0.96) and 3.7 ± 1.3 ns (fractional intensity, 0.04), respectively. As described above, the longer lifetime component with fractional intensity 0.04 was not due to background fluorescence. For a one-component analysis, χ^2 values were consistently larger. From 2 to 50 mol% cholestatrienol the lifetime values of τ_1 increased from 0.829 to 0.901 ns while τ_2 remained essentially constant in the analysis. However, the fractional intensity due to τ_2 decreased from 0.04 to 0.01.

Distributional lifetime analysis indicated consistently lower χ^2 values than discrete exponential analysis (table 2). Cholestatrienol (2 mol%) in POPC SUV had essentially a major component (average lifetime of 0.860 ns, width at half-height 0.05 ns) and a smaller, longer lifetime component near 3.24 ns. Increasing mol% cholestatrienol decreased the fractional intensity of the longer lifetime component from 0.04 (2 mol% choles-

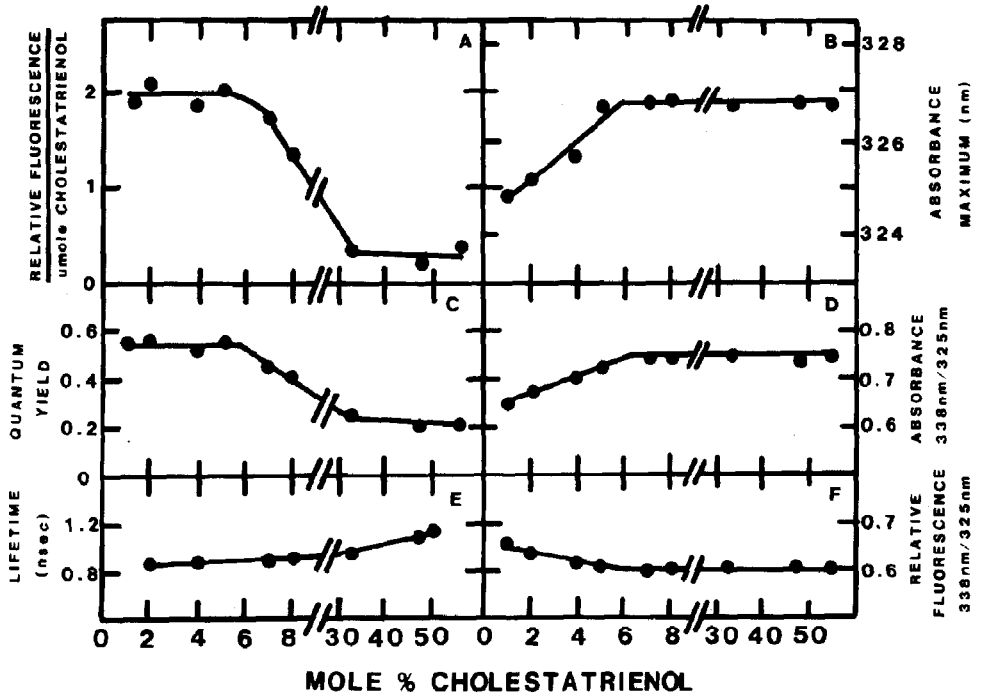

Fig. 3. Effect of increasing mol% cholestatrienol on fluorescence properties in POPC vesicles. All determinations were performed on intact SUV. The mol% cholestatrienol refers to the actual quantity of fluorescent sterol in the SUV (measured by HPLC and by fluorescence of the extracted neutral lipid fraction suspended in ethanol). (A) The relative fluorescence excitation intensity was determined at the fluorescence excitation maximum near 325 nm. (B) Absorbance spectra were determined with a Cary 210 ultraviolet/visible spectrometer. (C) Quantum yields at 325 nm were calculated at 24°C by comparison of fluorescence and absorbance of the fluorescent cholestatrienol relative to a standard, 1,6-diphenyl-1,3,5-hexatriene, in benzene (quantum yield = 0.80). (D) Absorbance spectra were obtained as for panel B. The ratio of the absorbance maximum near 338 nm to that near 325 nm was taken from these spectral scans. (E) Fluorescence lifetime at 325 was determined as described in section 2. Data represent only the major lifetime component (fractional fluorescence 0.96). (F) Fluorescence excitation spectra were obtained with the Spex Instruments photon counting fluorolog spectrofluorimeter. The ratio of the relative fluorescence intensity excitation maximum near 338 nm to the relative fluorescence excitation maximum near 325 nm was taken from these spectral scans.

tatrienol) to 0.00 (above 4 mol% cholestatrienol). The width at half-height of the two components was not changed. Increasing the mol% cholestatrienol increased the lifetime of the major component from 0.8 to about 1.1 ns. In summary, both exponential and distributional analysis indicate that in the range 2–4 mol% cholestatrienol in POPC SUV the cholestatrienol has essentially two lifetime components while at greater than 4 mol% cholestatrienol the proportion of the second, longer lifetime component decreased. To test whether this decrease was due to a segregation of sterol into separate domains above 4 mol% sterol in POPC SUV, a series of experiments were performed as described in the following sections.

3.4. Fluorescence spectral properties of cholestatrienol in POPC vesicles

The fluorescence emission at 376 nm when excited at 324 nm was determined for different concentrations of cholestatrienol in POPC SUV vesicles. The data plotted as relative fluorescence per μmol cholestatrienol vs. mol% cholestatrienol in the SUV (fig. 3A) indicate that relative fluorescence intensity/μmol cholestatrienol, but not relative fluorescence intensity (which decreased), was constant with increasing mol% cholestatrienol until about 6 mol%. Between 6 and 30 mol% the relative fluorescence/μmole cholestatrienol decreased approx. 75%. At greater than 30 mol%, the fluorescence of cholestatrienol decreased more slowly, apparently to a limiting value near 10% of the maximal value.

Three changes in absorbance at low mol% fluorescent sterol are also noted. First, for 0.5 mol% cholestatrienol the major absorption maximum in POPC SUV occurred at 324.9 nm; with increasing mol% fluorescent sterol the absorption maximum was red shifted. This shift was 1.8 nm near 6 mol% cholestatrienol. At higher sterol concentrations, no further shift was observed (fig. 3B). Second, there was a change in the ratio of absorbance at 338 nm to that at 325 nm (fig. 3D) from 0.66 to 0.73 and fluorescence excitation at 338 and 325 nm (fig. 3F) from 0.66 to 0.61. The ratio of absorbance at 338 nm/325 nm increased for cholestatrienol until 6 mol% fluorescent sterol. The ratio of fluorescence excitation peak intensities, in contrast, decreased (due to the lower fluorescence emission of this molecule at 338 nm than at 325 nm) until 6 mol% fluorescent sterol. Third, the absorbance at 325 nm increased linearly with increasing mol% cholestatrienol until about 6 mol% (data not shown). Since the absorbance at 325 nm and the relative fluorescence intensity at 325 nm both increased linearly with increasing mol% cholestatrienol up to 6 mol%, the cholestatrienol quantum yield should be constant between 0 and 6 mol% cholestatrienol. As shown in section 3.5, this was indeed the case.

3.5. Effect of cholestatrienol concentration in POPC SUV on quantum yield

The relative quantum yield of cholestatrienol in POPC SUV (fig. 3C), measured relative to diphenylhexatriene in benzene (quantum yield 0.80 at 24° C), was constant near 0.53, up to 6 mol% fluorescent sterol (fig. 3E). At concentrations higher than 6 mol% fluorescent sterol, the relative quantum yield decreased to a nonzero limiting value of 0.20 near 33 mol% sterol. In contrast, as described above, between 0 and 50 mol% cholestatrienol the lifetime of cholestatrienol did not decrease. This suggests a highly efficient quenching process for cholestatrienol above 6 mol% cholestatrienol.

3.6. The red edge effect

The steady-state fluorescence anisotropy of cholestatrienol was constant up to 6 mol% fluorescent sterol in POPC SUV (fig. 4A). This result is not consistent with sterol-sterol aggregation below 6 mol% sterol. The steady-state anisotropy of cholestatrienol decreased from 0.210 at 6 mol% to 0.113 at 33 mol%. At higher (above 33 mol%) concentrations of cholestatrienol the steady-state anisotropy reached a limiting value near 0.106. If depolarization is caused by homotransfer between cholestatrienol molecules (self-quenching), then this depolarization should be eliminated by excitation at the red edge of the absorption spectrum [2,6,39,40]. The data in table 4 indicate that cholestatrienol concentration quenching resulting

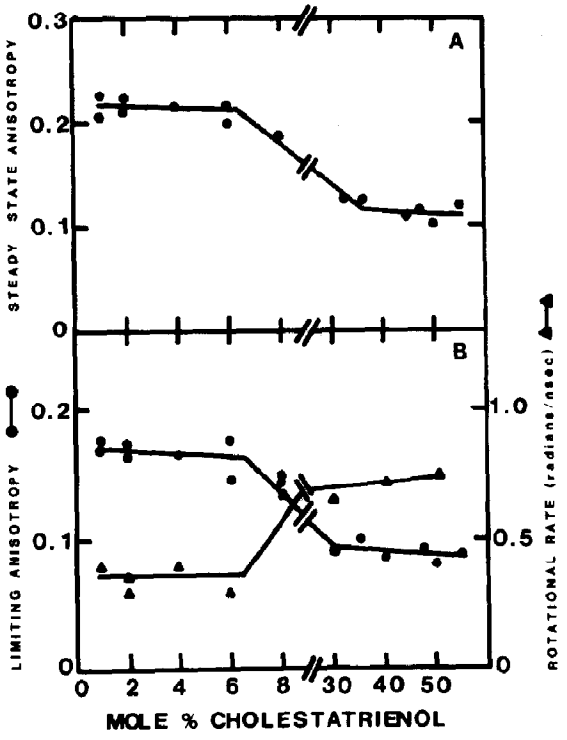

Fig. 4. Effect of mol% cholestatrienol on anisotropy and rotational rate of cholestatrienol in POPC vesicles. (A) Steady-state anisotropy was measured using the T-format SLM fluorimeter as described in section 2. (B) All parameters were determined by multifrequency phase and modulation techniques at 14 different frequencies as described in section 2. Limiting anisotropy (●———●); rotational rate (▲———▲).

in decreased anisotropy was noted both at the red edge of the absorption spectrum (356 nm) and at the major absorption maximum (325 nm), indicating the absence of a red edge effect and the absence of homotransfer.

Table 3

The red-edge effect for cholestatrienol self-quenching in POPC SUV

Fluorescence emission was measured at 376 nm. Values represent the mean ± S.E. ($n = 3$).

mol%		Steady-state anisotropy	
Cholestatrienol	POPC	325 nm	356 nm
2	98	0.210 ± 0.004	0.203 ± 0.003
42	48	0.109 ± 0.002	0.112 ± 0.003
55	45	0.102 ± 0.001	0.105 ± 0.003

3.7. *Dependence of limiting anisotropy and rotational rate on cholestatrienol concentration*

The limiting anisotropy of cholestatrienol (0.5 mol%) of POPC SUV was determined with the multifrequency (1–250 MHz) phase and modulation instruments using 14 different frequencies (10, 20, 30, 40, 60, 70, 80, 90, 100, 115, 120, 130, 140 and 150 MHz). The limiting anisotropy thereby obtained and the rotational rate calculated according to the equations developed by Lakowicz et al. [36] were 0.170 and 0.41 radian/ns, respectively, at 24° C (fig. 4B). Thus, cholestatrienol appears highly ordered with a restricted range of rotation but rapid rate of motion in POPC membrane bilayers. The limiting anisotropy parameter was constant up to 6 mol% cholestatrienol and then decreased with increasing mol% fluorescent sterol to nonzero limiting values near 0.098 for at 33 mol% cholestatrienol (fig. 4B). Concomitant to the decrease in limiting anisotropy was a faster rotational rate near 0.75 radian/ns (shorter rotational relaxation time).

3.8. *Effect of cholesterol on fluorescence properties of cholestatrienol in POPC vesicles*

The similarity of cholesterol and cholestatrienol structural and dynamic properties in POPC SUV was examined using a low concentration of cholestatrienol (3 mol%) and increasing cholesterol (0–17 mol%) in POPC SUV. The relative fluorescence intensity of 3 mol% cholestatrienol was constant with increasing mol% cholesterol (not shown) in the range 0–7 mol%. As expected, above 8 mol% total sterol the relative fluorescence intensity/μmol total sterol decreased to a limiting value (fig. 5A). Between 0 and 8 mol% total sterol, the major absorbance maximum near 324.7 nm was red shifted (fig. 5B) and the ratio of absorbance at 338 nm/324 nm increased (fig. 5C). These observations are very similar to those obtained above with POPC SUV containing only increasing concentrations of cholestatrienol between 0 and 6 mol% (fig. 3A, B and D).

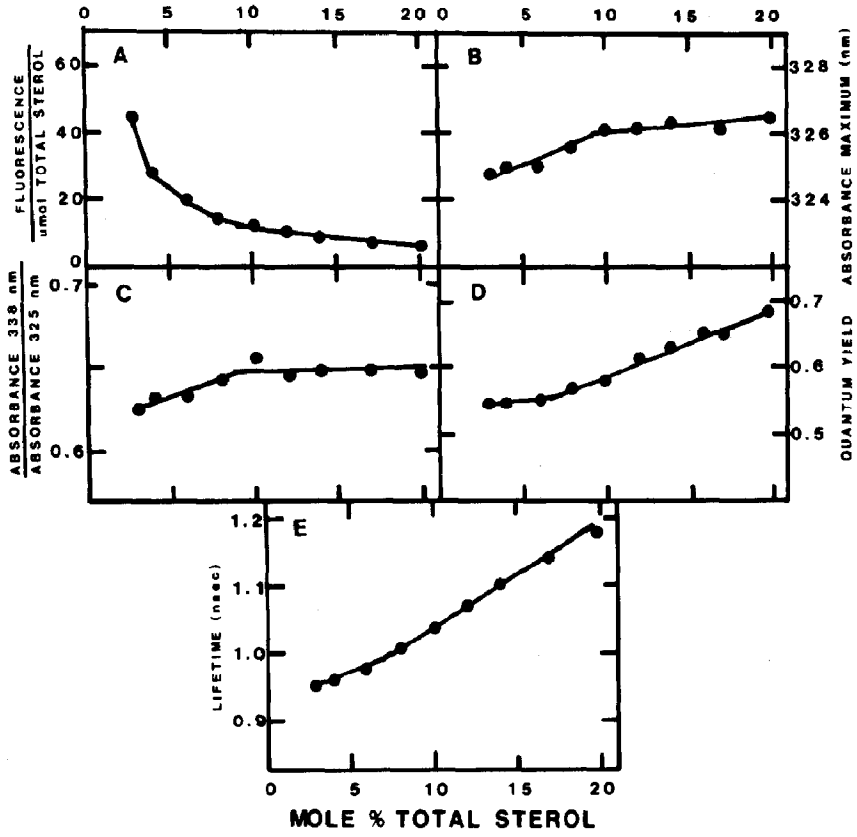

Fig. 5. Effect of cholesterol on fluorescence properties of cholestatrienol in POPC vesicles. POPC SUV contained 3 mol% cholestatrienol and 0–17 mol% cholesterol. Lifetime data were obtained using phase and modulation data at eight frequencies and analyzed by continuous distributional analysis to two lifetime components. Data for only the major component are shown. Absorbance spectra were recorded with a Gilford spectrophotometer. Other parameters were determined as described in section 2.

Increasing the cholesterol content of the POPC SUV (up to 6 mol% total sterol) did not significantly change the quantum yield (fig. 5D) or the fluorescence lifetime (fig. 5E) of 3 mol% cholestatrienol. Analysis of lifetime data for a two-component fit resulted in χ^2 values between 0.3 and 2.9 (fig. 5E). The steady-state anisotropy, limiting anisotropy and rotational rate of cholestatrienol were essentially unaltered between 0 and 8 mol% total sterol (fig. 6A–C). At sterol concentrations above 8 mol% total sterol, the quantum yield (fig. 5D) and lifetime both increased. In POPC vesicles containing 50 mol% cholesterol, these increases for cholestatrienol were even greater (data not shown). The steady-state anisotropy (fig. 6A) and limiting anisotropy (fig. 6B) of low concentrations of cholestatrienol (0.5 or 3 mol%) in POPC SUV increased when the total sterol content was increased from 10 to 20 mol%. Concomitantly, the rotational rate decreased from 0.55 to 0.25 radian/ns. These results indicate that the addition of cholesterol above 8 mol% total sterol restricts both the range and rate of motion of the fluorescent sterol in the POPC SUV.

In summary, cholestatrienol and cholesterol appear to have a similar effect on cholestatrienol fluorescence parameters explained by dielectric changes at low mol% total sterol (see section 4). With increasing mol% cholestatrienol in the range 0–6 mol%, the fluorescent sterol senses a more polar environment in the sterol-poor domain. At higher mol% total sterol the added cholesterol

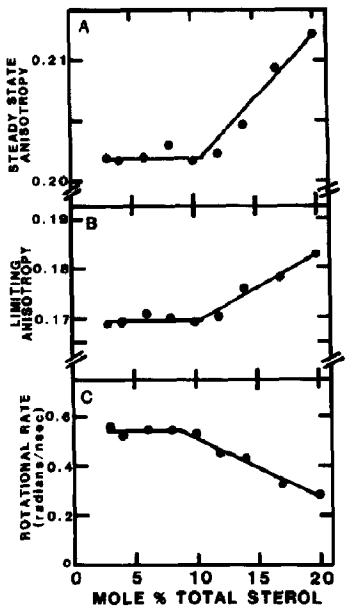

Fig. 6. Effect of cholesterol on dynamic and static properties of cholestatrienol in POPC vesicles. All conditions were as described in the legend to fig. 5. Steady-state anisotropy (A), limiting anisotropy (B), and rotational rate (C) were determined as described in section 2 using phase and modulation data at eight frequencies. The limiting anisotropy and rotational rate were calculated, using a floating value for r_0, also as described in section 2.

orders the laterally segregated sterol domain (figs. 5 and 6). In contrast, high mol% cholestatrienol results in quenching and indicates that the sterol-poor sterol (nonsegregated) domain, where the remaining signal is observed, becomes more disordered.

4. Discussion

4.1. Polarity sensitivity of cholestatrienol in POPC SUV

4.1.1. Properties of cholestatrienol at low mol% in POPC SUV

Several observations obtained with the fluorescent cholestatrienol indicate that at low mol% in POPC SUV this sterol is sensitive to dielectric effects. At concentrations up to about 6 mol% cholestatrienol in the POPC bilayer, the absorbance maximum of cholestatrienol near 325 nm was red shifted 1.8 nm. The ratio of the cholestatrienol (fig. 3D) and dehydroergosterol [2] absorbance peak maxima increased in the concentration range 0–6 mol%. A similar 1.4 nm red shift was observed for 5 mol% dehydroergosterol, another fluorescent sterol, in POPC SUV [2]. In contrast, the ratio of the relative fluorescence excitation of cholestatrienol (fig. 3B) and cholesterol [2] near 338 nm to the relative fluorescence excitation near 324 nm also increased in the concentration range 0–6 mol%.

In the presence of 3 mol% cholestatrienol addition of cholesterol from 0 to 5 mol% cholesterol also red shifted the absorbance maximum and altered absorbance peak ratios of cholestatrienol (fig. 5) and dehydroergosterol [2]. Since fluorescence lifetime and quantum yield were constant between 0 and 6 mol% cholestatrienol or dehydroergosterol, these shifts were not due to cholestatrienol aggregation and self-quenching at low mol% sterol. If cholestatrienol or dehydroergosterol are good analogues for cholesterol, then self-quenching of laterally segregated cholestatrienol is not expected with increasing concentration of cholesterol in the range 0–6 mol%. The absence of anisotropy changes rules out aggregation of cholestatrienol below 6 mol%. The above observations may be explained by dielectric constant effects. The addition of cholestatrienol, dehydroergosterol [2], or cholesterol can cause a change of the average dielectric properties of the POPC membrane microenvironment wherein the fluorophore is located. Space-filling models of cholesterol (and cholestatrienol) indicate that the conjugated triene double-bond series of cholestatrienol is located within a few ångströms of the OH group. In phosphatidylcholine SUV membranes the fluorescence intensity and lifetime of cholestatrienol are strongly dependent on the dielectric constant of the membrane microenvironment. The data are consistent with the interpretation that with increasing concentration up to 6 mol% cholestatrienol in the POPC vesicles, there is a linear change of the membrane microenvironment dielectric constant.

4.1.2. Multiple lifetimes of cholestatrienol in POPC SUV

Lifetime data analysis by Lorentzian distri-

bution of lifetimes is also consistent with polarity sensitivity of cholestatrienol. Below 6 mol% cholestatrienol two lifetime components of fractional intensity near 0.96 and 0.04, were resolved by continuous distributional as well as exponential analysis. As indicated by reduced χ^2, the distributional analysis gave as a good or a better fit than the exponential analysis. Although there is no reason to expect that the real lifetime distributions are symmetric, the analysis is easier and more rapid assuming symmetric distributions. Heterogeneity of vesicle preparations cannot explain the observed lifetime distributions. The longer lifetime component of cholestatrienol in different sized vesicles has lifetime values differing by as much as 0.4 ns (3.24 ns in SUV and 2.80 ns in multilamellar vesicles). If the lifetime of cholestatrienol in each vesicle size is a single exponential, the size heterogeneity will give rise to a lifetime distribution within a 0.4 ns range. The summation of single exponentials over the range 0.4 ns would result in a distribution that is the same as a single exponential. If the decay of cholestatrienol is assumed to be best explained by a Lorentzian distribution, the lifetime changes may be explained. At least two factors must be considered to explain qualitatively the origin of such a distribution of lifetime values and alterations therein. First, it is assumed that cholestatrienol molecules exist in a distribution of environments. The cholestatrienol is sensitive to the dielectric constant of the medium wherein it resides. If cholestatrienol can be located at different positions along the bilayer normal and the membrane polarity of the surface and interior differs markedly, a range of lifetimes should exist for the cholestatrienol in the POPC SUV. Second, if the translational diffusion rate is the same or faster than the lifetime, then the cholestatrienol will rapidly average over the different environments. The lateral diffusion rate of NBD-cholesterol, another fluorescent sterol derivative, is very rapid, 2×10^{-10} cm^2 s^{-1} [39]. At lower sterol content, the average lifetime should then decrease since the cholestatrienol molecule will be in a microenvironment with a more rapid decay during its fluorescence lifetime. In addition, the distribution should be narrow because the lifetime value is determined by the average environment. It is also assumed that interconversion occurs between environments. When the interconversion rate is fast (e.g., low mol% sterol), the cholestatrienol molecule averages different positions in the membrane during the excited-state lifetime resulting in a narrow distributional width. Indeed, the data for cholestatrienol at low mol% sterol show shorter lifetime and a narrow distributional width (0.05 ns). Similar results have been observed for diphenylhexatriene in phosphatidylcholine SUV [20,21]. In summary, the distributional analysis of cholestatrienol in POPC SUV (below 6 mol% cholestatrienol) is consistent with the presence of two populations of sterol: a small portion (0.04 fractional fluorescence) resides in a microenvironment of greater polarity (longer lifetime) than a second much larger component (shorter lifetime).

4.1.3. Other fluorescent sterols

The proposal that sterols in membranes may be sensitive to dielectric effects is consistent with data reported for dehydroergosterol (2) and *N*-(2-naphthyl)-23,24-dinor-5-cholen-22-amin-3β-ol [41]. The fluorescence properties of this fluorescent sterol were also solvent polarity sensitive. The hydrocarbon region of the bilayer sensed by this fluorophore had a polarity comparable to that of acetonitrile. This polarity was reduced by addition of increasing amounts of cholesterol. This result appears opposite to that obtained for cholestatrienol and dehydroergosterol [2] whose red-shifted absorbance maximum with increased cholesterol indicates an increased polarity. These differences may be reconciled by recognizing that the naphthyl group was located at the cholesterol alkyl chain, the opposite end of the sterol molecule from where the cholestatrienol and dehydroergosterol fluorophores are located. The naphthylcholesterol should therefore probe more deeply the bilayer core. The naphthylcholesterol [41] may preferentially partition into sterol-rich, more hydrophobic domains or perhaps even laterally segregate from cholesterol. In contrast, the cholestatrienol and dehydroergosterol [2] do not appear to show such preference.

Another napthylcholesterol derivative was recently synthesized and characterized [42,43]. When placed in large unilamellar phospholipid vesicles,

the fluorescence lifetime properties of this derivative also altered dramatically near 7 mol% [44]. A phase diagram of cholesterol in phospholipid vesicles based on NMR and DSC results also showed a break near 6–8 mol% cholesterol [45]. From these data it may be suggested that above 6–8 mol% cholestatrienol, the sterols partially segregate into sterol-rich but not pure sterol domains. A pure sterol phase does not phase separate until 50–67 mol% cholesterol [46]. In conclusion, below 6 mol% the sterol molecules appear more sensitive to polar effects than at greater mol% sterol, possibly due to being inserted into the bilayer less deeply or the lipid polar head groups occupying more area and allowing greater penetration of H_2O. Either effect would result in a greater interaction of the fluorescent sterol fluorophore with the aqueous interface (higher dielectric constant) below 6 mol% sterol. The molecular origins of this phenomenon and why it disappears near 6 mol% sterol are not known. One simple explanation might be that cholesterol and cholestatrienol insert themselves into the liquid crystalline (fluid) POPC bilayer in a highly specific fashion which leads to a condensing or ordering effect. This would be expected to reduce the number of vacancies occurring in the bilayer and consequently to reduce the permeability of the bilayer to water and small molecules.

4.2. Dynamic properties of sterol-rich and sterol-poor domains in fluid-phase POPC SUV

4.2.1. The sterol-poor domain at low mol% sterol

The data presented here for increasing mol% sterol are consistent with the presence of a sterol-poor, possibly monomeric, domain that is polarity sensitive. As demonstrated above, between 0 and 6 mol% the sterols do not interact as indicated by the absence of decreased lifetime resulting from cholestatrienol quenching. The data presented here indicate that at greater than 6 mol% cholestatrienol partially separates to quench fluorescence. Such a phase separation is also consistent with observations made for chlorophyll *b* self-quenching [41]. Therefore, above 6 mol% cholestatrienol or dehydroergosterol [2] the observed fluorescence signal is due to the nonphase-separated, sterol-poor domain. Above 33% cholestatrienol or dehydroergosterol [2] the steady-state anisotropy and limiting anisotropy decreased to limiting values while rotational rate increased. Thus, the sterol-poor domain (0–6 mol%) became more disordered (or fluid) at sterol concentrations sufficiently high for sterol phase separation (above 6 mol%).

4.2.2. Formation of sterol-rich domains

The results presented here suggest that above 6 mol% cholestatrienol the additional sterol laterally segregates into a sterol-rich but not pure sterol domain. The lack of a red-edge effect at high cholestatrienol concentration indicates that lateral segregation into pure sterol-containing domains is unlikely. Indeed, other investigators have shown that in the fluid state, the maximum amount of cholesterol accommodated in phospholipids before a pure cholesterol phase separates out is 50–67 mol%, depending on the phospholipid polar head group [46]. Thus, the data presented here and by others are consistent with the possibility that between 5 and 50 mol% sterol, sterol-rich (but not pure sterol) domains segregate laterally within the membrane. Results from a number of investigators [2,44,45,47] are consistent with this interpretation. A key observation in this regard is the presentation of a phase diagram for cholesterol in phospholipid multilamellar vesicles indicating not only a phase separation near 6–8 mol% cholesterol but also the presence of cholesterol in ordered and disordered fluid domains [45]. The data obtained for cholestatrienol and dehydroergosterol [2] both indicate that a relatively disordered (fluid) sterol domain exists. In addition, a second much larger phase-separated domain that is more ordered is present above 6 mol% sterol (fig. 6; also ref. 2). Above 6 mol% sterol, both domains coexist in POPC SUV at 24 °C, a temperature at which POPC is in the fluid phase. Evidence for fluid-fluid phase immiscibility was previously presented for phospholipids. For example, when POPC (the major component of egg PC), egg PC, and dimyristoylphosphatidylcholine are all in the fluid state, it has been postulated that above 5 mol% cholesterol, coexisting, immiscible fluid domains may be present under certain conditions [39,47]. Fluid-fluid immiscibility was also obtained in bi-

nary mixtures of dipalmitoylphosphatidylethanolamine and dielaidoylphosphatidylcholine [48]. Electron spin resonance data are consistent with the formation of cholesterol-rich and cholesterol-poor domains in biological membranes [49,50]. The existence of a long-lived cholesterol-lipid complex that may form near 4 mol% cholesterol has been postulated [2,19,51–53]. Cholesterol association with the more fluid phase in phase-separated systems has been predicted in phase-separated disaturated/ disaturated and disaturated/ monounsaturated phosphatidylcholine mixtures [54,55]. Above 25 mol% cholesterol, spin-labeled steroids were no longer completely miscible with dipalmitoylphosphatidylcholine membranes [56]. X-ray investigations indicated that below 50 mol% cholesterol, a ribbon-like structure was noted below the phase transition of dipalmitoylphosphatidylcholine corresponding to cholesterol-poor and cholesterol-rich areas [57]. However, these structures still allowed phospholipid-sterol interactions. The data presented herein for cholestatrienol and earlier for dehydroergosterol [2] are consistent with the interpretation that cholesterol-rich and cholesterol-poor areas may also exist above the phase transition of phospholipids.

4.3. Dynamic and static properties of cholestatrienol in sterol-rich and sterol-poor domains of POPC SUV

At low mol% cholestatrienol has a fast rotational relaxation time (0.27 ns) and a high degree of order in liquid-crystalline POPC SUV at 24 °C. These findings are consistent with those of other investigators obtained by deuterium NMR of deuterated cholesterol in multilayers of egg phosphatidylcholine: order parameters and rotational relaxation times were near 0.67 and 0.5 ns, respectively [58,59]. In contrast, in the phase-separated sterol domain obtained at high mol% sterol (greater than 6 mol%) the order parameter of deuterated cholesterol was increased to 0.78 in egg phosphatidylcholine multilayers [60], 0.80 in dimyristoylphosphatidylcholine and 0.76 in human erythrocyte ghosts [53]. Similarly, the results presented here show that the limiting anisotropy (which reflects order S, according to $S = (r_\infty/r_0)^{1/2}$) of cholestatrienol (3 mol% plus 3–17 mol% cholesterol) in POPC SUV increased in the cholesterol-rich domain. The amplitude determined from the limiting anisotropy and rate of anisotropic motion are not necessarily correlated. The results obtained with cholestatrienol herein and earlier with dehydroergosterol [2] indicate that cholesterol increased both the lifetime and the rotational relaxation time of the fluorescent sterol in POPC SUV.

4.4. Conclusion

The fluorescent sterol cholestatrienol is a useful probe molecule analogue for cholesterol. In POPC SUV it appears quite sensitive to dielectric effects below 6 mol% and to sterol interactions with other sterols and/or lipids above 6 mol% sterol. The fluorescent sterol is sensitive to the presence of two sterol-containing domains. In addition, it is an excellent probe molecule for examining the motional properties (dynamic and static) of cholesterol in model phospholipid membranes. The motional properties of the fluorescent sterol indicate rapid motion (dynamics) with a restricted degree of rotation (order) in the sterol-poor domain. Both parameters indicate increased disorder in this domain in the presence of a sterol-rich domain at high mol% cholesterol in the POPC vesicles. In contrast, the sterol-rich domain becomes increasingly ordered at higher mol% sterol in POPC SUV. The data obtained herein with cholestatrienol are in good agreement with those obtained with dehydroergosterol [2,19,52], indicating that both molecules appear to be appropriate analogues for cholesterol in membrane studies.

Acknowledgements

The authors would like to acknowledge the expert technical assistance of Mr. Eugene Hubert. We wish to thank Dr. P. Holloway, Department of Biochemistry, University of Virginia, for the use of the Aminco-Bowman spectrophotometer, Dr. C. Kreutz, Department of Pharmacology, University of Virginia, for the use of his Spex Fluorolog

spectrofluorimeter, and Dr. Carol Caperelli, Division of Pharmacology and Medicinal Chemistry, University of Cincinnati, for use of the Cary 210 spectrophotometer.

This work was supported in part by grants from the USPHS (GM 31651 and AA 07292, F.S.; GM-14628, T.E.T.; HL 17576, U.S. Israel BSF 2669 and 2772, Y.B.), and USPHS (1P41 RR 03351, E.G.).

References

1 F. Schroeder, Prog. Lipid Res. 23 (1984) 97.
2 F. Schroeder, Y. Barenholz, E. Gratton and T.E. Thompson, Biochemistry 26 (1987) 2441.
3 A.B. Kier, W.D. Sweet, M.S. Cowlen and F. Schroeder, Biochim. Biophys. Acta 861 (1986) 287.
4 J.E. Hale and F. Schroeder, Eur. J. Biochem. 122 (1982) 649.
5 F. Schroeder, FEBS Lett. 135 (1981) 127.
6 J. Rogers, A.G. Lee and D.C. Wilton, Biochim. Biophys. Acta 552 (1979) 23.
7 D.B. Archer, Biochem. Biophys. Res. Commun. 66 (1975) 195.
8 D. Sica, L. Boniforti and G. DiGiacomo, Phytochemistry 21 (1982) 234.
9 P.L. Yeagle, J. Benson, M. Greco and C. Arena, Biochemistry 21 (1982) 1249.
10 P. Child and A. Kuksis, J. Lipid Res. 24 (1983) 1196.
11 R.T. Fischer, F.A. Stephenson, A. Shafiee and F. Schroeder, J. Biol. Phys. 13 (1985) 13.
12 R.T. Fischer, F.A. Stephenson, A. Shafiee and F. Schroeder, Chem. Phys. Lipids 36 (1984) 1.
13 T. Parasassi, F. Conti, M. Glaser and E. Gratton, J. Biol. Chem. 259 (1977) 14011.
14 L.A. Sklar, B.S. Hudson and R.D. Simoni, Biochemistry 16 (1977) 819.
15 F. Schroeder, Eur. J. Biochem. 132 (1983) 509.
16 F. Schroeder, I.E. Goetz and E. Roberts, J. Neurochem. 43 (1984) 526.
17 P.K. Wolber and B.S. Hudson, Biochemistry 20 (1981) 2800.
18 T. Parasassi, F. Conti and E. Gratton, Biochemistry 23 (1984) 5660.
19 G. Smutzer, B.F. Crawford and P.C. Yeagle, Biochim. Biophys. Acta 862 (1986) 361.
20 R. Fiorini, M. Valentino, S. Wang, M. Glaser and E. Gratton, Biochemistry 26 (1987) 3864.
21 R.M. Fiorini, M. Valentino, E. Gratton, E. Bertoli and G. Curatola, Biochem. Biophys. Res. Commun. 147 (1987) 460.
22 D.R. James, J.R. Turnbull, B.D. Wagner, W.R. Ware and N.O. Petersen, Biochemistry 26 (1987) 6272.
23 Y. Barenholz, D. Gibbes, B.J. Litman, J. Goll, T.E. Thompson and F.D. Carlson, Biochemistry 15 (1977) 2806.
24 F. Schroeder, J.F. Perlmutter, M. Glaser and P.R. Vagelos, J. Biol. Chem. 251 (1976) 5015.
25 B.R. Lentz, B.M. Moore and D.A. Barrow, Biophys. J. 25 (1979) 489.
26 C.S. Chong and K. Colbow, Biochim. Biophys. Acta 436 (1976) 260.
27 R.F. Chen and R.L. Bowman, Science 147 (1965) 729.
28 E. Gratton and M. Limkeman, Biophys. J. 44 (1983) 315.
29 R.A. Spencer and G. Weber, Ann. N.Y. Acad. Sci. 158 (1969) 361.
30 J.R. Lackowicz, G. Laczko, H. Cherek, E. Gratton and M. Limkeman, Biophys. J. 46 (1984) 463.
31 J.R. Lakowicz, G. Laczko, H. Cherek, E. Gratton and E. Limkeman, Biophys. J. 46 (1984) 463.
32 M.S. Caceri and W.P. Cacheris, Byte 9 (1980) 340.
33 E. Gratton, D.M. Jameson, R. Hall, Annu. Rev. Biophys. Bioeng. 13 (1984) 105.
34 G. Weber, Acta Phys. Pol. A54 (1978) 859.
35 J.R. Lakowicz, E. Gratton, H. Cherek, B.P. Maliwal and G. Laczko, J. Biol. Chem. 259 (1984b) 10967.
36 J.R. Lakowicz, F.G. Prendergast, and D. Hogen, Biochemistry 18 (1979) 508.
37 M. Shinitzky and Y. Barenholz, J. Biol. Chem. 249 (1974) 2652.
38 R. Antonucci, S. Bernstein, D. Giancola and K.J. Sax, J. Org. Chem. 16 (1951) 1159.
39 M.R. Alecio, D.E. Golan, W.R. Veatch and R.R. Rando, Proc. Natl. Acad. Sci. U.S.A. 79 (1982) 5171.
40 A.R. Kelly and L.K. Patterson, Proc. Roy. Soc. Lond. A. 324 (1971) 117.
41 Y.J. Kao, A.K. Soutar, F.-Y. Hong, H.J. Pownall and L.C. Smith, Biochemistry 17 (1978) 2689.
42 J. Drew, J.-R. Brisson, P. Morand and A.G. Szabo, Can. J. Chem. 65 (1987) 1784.
43 J. Drew, M. Letellier, P. Morand and A.G. Szabo, J. Org. Chem. 52 (1987) 4047.
44 J. Drew, A.G. Szabo and P. Morand, in: Time-resolved laser spectroscopy in biochemistry, ed. J.R. Lakowicz (SPIE Press, 1988) Vol. 909, p. 299.
45 H.J. Ipsen, G. Karlstrom, O.G. Mouritsen, H. Wennerstrom and M.J. Zuckermann, Biochim. Biophys. Acta 905 (1987) 162.
46 M.D. Houslay and K.K. Stanley, in: Dynamics of biological membranes, eds. M.D. Houslay and K.K. Stanley (Wiley, New York, 1982) p. 75.
47 B.R. Lentz, D.A. Barrow and M. Hoechli, Biochemistry 19 (1980) 1943.
48 D.E. Golan, M.R. Alecio, W.R. Veatch and R.R. Rando, Biochemistry 23 (1984) 332.
49 S.H.W. Wu and H.M. Mcconnell, Biochemistry 14 (1975) 847.
50 L.M. Gordon and P.W. Mobley, J. Membrane Biol. 79 (1984) 75.
51 L.M. Gordon, P.W. Mobley, J.A. Esgate, G. Hofmann, A.D. Whetton and M.D. Houslay, J. Membrane Biol. 76 (1983) 139.

52 P.L. Chong and T.E. Thompson, Biochim. Biophys. Acta 863 (1986) 53.
53 D.J. Recktenwald and H.M. McConnell, Biochemistry 20 (1981) 4505.
54 M.C. Phillips and E.G. Finer, Biochim. Biophys. Acta 356 (1974) 199.
55 A.J. Verkleij, P.H.J.T. Ververgaert, B. de Kruyff and L.L.M. van Deenen, Biochim. Biophys. Acta 373 (1974) 495.
56 B. de Kruyff, P.W.M. van Dijck, R.A. Demel, A. Schuijff, F. Brants and L.L.M. van Deenen, Biochim. Biophys. Acta 356 (1974) 1.
57 H. Trauble and E. Sackmann, J. Am. Chem. Soc. 94 (1972) 4499.
58 S.W. Hui and D.F. Parsons, Science 190 (1975) 383.
59 M.G. Taylor, T. Akiyama and I.C.P. Smith, Chem. Phys. Lipids 29 (1981) 327.
60 M.G. Taylor, T. Akiyama, H. Saito and I.C.P. Smith, Chem. Phys. Lipids 31 (1982) 359.
61 E.C. Kelusky, E.J. Dufourc and I.C.P. Smith, Biochim. Biophys. Acta 735 (1983) 302.